JOURNAL OF MATERIALS SCIENCE 24 (1989) 3146–3153

The corrosion of glass on the sea bed

G. A. COX, B. A. FORD
Department of Physics, University of York, York YO1 5DD, UK

Alkali-lime-silicate glasses, which have corroded on the sea bed for approximately 240 years, have been studied using scanning electron microscopy, electron-probe microanalysis, X-ray and electron diffraction, and infrared spectroscopy to quantify the nature of the decay processes. Leaching and dissolution of the glass network occurs, followed by reprecipitation of new phases to produce corrosion crusts consisting of discrete layers of striking regularity. Depth profiles of the elements in the crusts revealed them to be depleted of calcium and magnesium. Silicon was enriched at the glass–corrosion interface; aluminium was concentrated throughout the crusts; iron and sulphur were enriched at the exposed surfaces. Sodium and potassium showed less regular behaviour. Several crystalline phases were identified amongst the corrosion products, not all of which arose from the decomposition of the glass.

1. Introduction

The corrosion and decay of glass in the natural environment is a subject of considerable technological importance, because the preferred method of high-level nuclear waste disposal is to vitrify it then, after encapsulation, to bury it in a stable geological formation. In time, the waste canisters will lose their integrity, allowing groundwater to come into contact with the glass, when leaching and other processes will occur, resulting in the release of radionuclides into the environment. Much work is being done to simulate the hydrothermal conditions which will prevail in a nuclear waste repository and to study the behaviour of glass in such a situation. Most of this research has concentrated on short-term accelerated corrosion experiments carried out at elevated temperatures in the laboratory, with the objective of predicting the long-term stability of the glass.

The phenomenon of glass corrosion in the natural environment over long periods of time is well known to glass scientists and archaeologists. That decomposed glass often has an iridescent, laminated appearance was reported by Brewster in 1863 [1]. Raw [2], Geilmann [3] and Newton [4] have subsequently investigated this subject. Attempts have been made to determine the date of burial of ancient glass based upon details of the corrosion crust [5]; the age of obsidian, a volcanic glass, may be estimated by measuring the thickness of the surface hydration layer [6]. Not surprisingly, there has been some interest in using naturally corroded glasses as models for nuclear waste glass [7], but comparatively little quantitative work has been reported in this field. Research was therefore commenced at the University of York to study environmentally corroded glass from a variety of archaeological sites – both marine and land-based – and to obtain quantitative data on the morphology and composition of the corrosion products. In this paper we report observations made on glass which has corroded on the sea bed for approximately 240 years.

2. Material and methods

Glass from two in-shore shipwrecks has been studied: (i) the *Drottengin af Sverige*, which sank off Lerwick harbour, the Shetland Islands in 1745, and (ii) the Dutch East Indiaman *Amsterdam*, which foundered off Hastings, in 1749 [8].

Much glass was recovered from these sites, mostly in the form of fragments of vessels. All the pieces examined were mid-green in colour and had an opaque corrosion crust, approximately 0.2 to 0.5 mm thick, which was extremely fragile. Its colour was orange-yellow on material from the *Drottengin af Sverige* (specimens designated DS), and red-brown on that from the *Amsterdam* (specimens designated AMS). A fragment from the former wreck in the as-received state is illustrated in Fig. 1.

Areas of the corrosion crust were mechanically removed and coated with carbon for examination in the scanning electron microscope (SEM). A Cambridge Instruments S90B microscope was used fitted with a Link Systems AN10000 energy dispersive X-ray analyser to permit electron probe microanalysis (EPMA) to be carried out. The operating conditions were 15 kV accelerating voltage and 0.5 nA beam current. Corrected quantitative chemical analyses were obtained by subjecting net fluorescent X-ray intensities from the elements of interest to a ZAF computer program [9].

Selected specimens were carefully sectioned using a diamond saw and mounted in "Epoxide" resin (Buehler). The fragile corrosion crust was preserved intact by first consolidating it with a 5% solution of "Acryloid" B-72 (Rohm & Haas Co.) in acetone. The embedded sections were ground flat and polished with diamond paste to a $\frac{1}{4}\,\mu$m finish. Such specimens were initially studied at low magnification with an optical microscope; later they were examined in the SEM after being coated with carbon.

Small areas of the crusts were removed for diffraction studies. Electron diffraction was carried out on a

0022–2461/89 $03.00 + .12

Figure 1 Specimen DS1 in the as-received state showing the corroded surface and the pristine glass.

Hitachi HU-11E transmission electron microscope, whilst X-ray diffraction patterns were obtained from powdered samples using a Phillips PW 1024/30 camera and filtered CuK_α radiation.

Infrared (IR) absorption spectra of the glass and corrosion products were recorded using a Perkin–Elmer spectrophotometer, model 580. Finely powdered samples were mixed with high-purity potassium bromide and pressed into thin discs.

3. Results

3.1. Composition of the glasses

The chemical composition of the unaltered glass was determined by EPMA for several specimens. The results are presented in Table I. All of the glasses have relatively low total alkali (Na_2O and K_2O) contents, but high concentrations of silica (SiO_2) and calcia (CaO). The DS specimens have somewhat higher potash (K_2O) and alumina (Al_2O_3) contents than the AMS specimens. In general, the glasses from the two sites are remarkably similar in composition, being of the (mixed) alkali-lime-silicate type.

3.2. Surface studies

The surfaces of the corrosion crusts proved to be most interesting – both the surface which had been exposed to the environment and that at the glass–corrosion interface. Their chemical compositions in the as-received state were determined for comparison with those of the pristine glass. The results are presented in Table II. They show a range of variability, but basically silicon is enriched at the glass–corrosion interface, whilst calcium and magnesium have largely been lost. Aluminium is greatly concentrated in the corrosion products relative to the unaltered glass. The sodium and potassium contents show less regular behaviour, possibly on account of the relatively high concentration of alkali ions in seawater, which would influence the diffusion of these mobile ions through the porous crusts. In the DS specimens the exposed surface was considerably enriched in sulphur; for the AMS specimens iron was concentrated at this surface.

Examination of the corrosion crusts in the SEM revealed much structural detail, those present on the *Drottengin af Sverige* material being particularly interesting. Fig. 2 shows a piece of the crust from specimen DS1 where a layer structure is apparent. This accounts for the extreme fragility of the specimens, especially when dry, and the ease with which the crust exfoliates. On the exposed surface of this specimen a number of unexpected features were observed.

Illustrated in Fig. 3 is a well-developed pseudo-hexagonal structure which EPMA revealed to be rich in calcium and sulphur (in wt %: Ca 27 to 30, S 22 to 25). Numerous other surface deposits with different regular forms occurred on this specimen, all of which

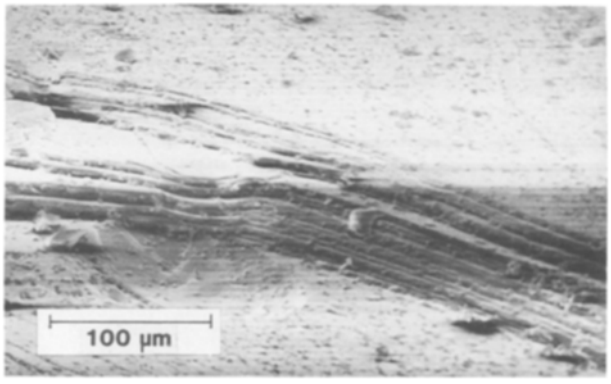

Figure 2 Scanning electron micrograph of corrosion layers on specimen DS1.

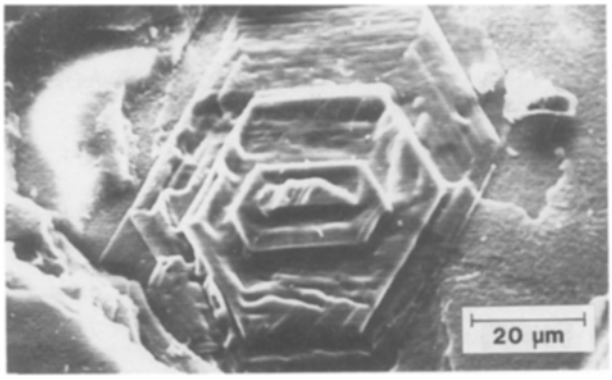

Figure 3 Deposit of gypsum on the exposed surface of the corrosion crust from specimen DS1.

TABLE I Composition of the glasses

Oxide	*Amsterdam*				*Drottengin af Sverige*			
	AMS1	AMS3	AMS4	AMS5	DS1	DS2	DS3	DS4
Na_2O	3.4	3.0	4.0	3.1	3.0	2.9	3.3	3.4
MgO	3.0	3.1	2.5	2.7	3.9	3.8	3.2	3.7
Al_2O_3	3.3	3.8	3.4	3.2	7.4	6.3	7.6	7.5
SiO_2	61.7	57.6	61.0	59.4	55.2	56.3	59.6	54.4
P_2O_5	2.4	2.4	2.3	2.3	2.0	1.8	1.9	1.5
K_2O	3.2	2.5	2.0	2.8	4.0	6.0	6.7	5.0
CaO	22.2	24.0	22.1	21.8	20.3	20.1	19.5	19.0
MnO	0.7	0.6	0.5	0.9	1.1	1.2	1.2	1.1
Fe_2O_3	1.2	1.3	1.2	1.2	1.5	1.6	1.9	1.8
S	ND	0.4	ND	ND	0.1	ND	ND	0.1
Cl	0.7	0.8	1.2	0.7	ND	ND	ND	0.5

ND Not detected.

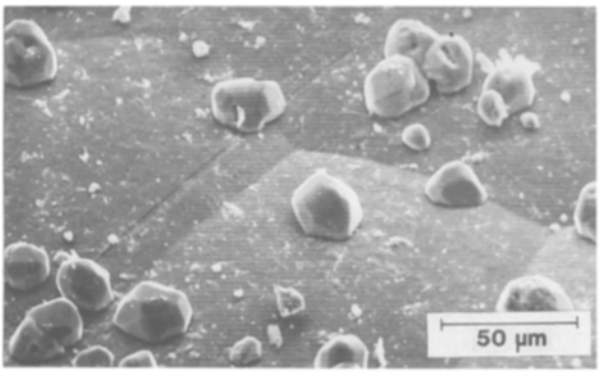

Figure 4 Sulphur crystals on the exposed surface of the corrosion crust from specimen DS4.

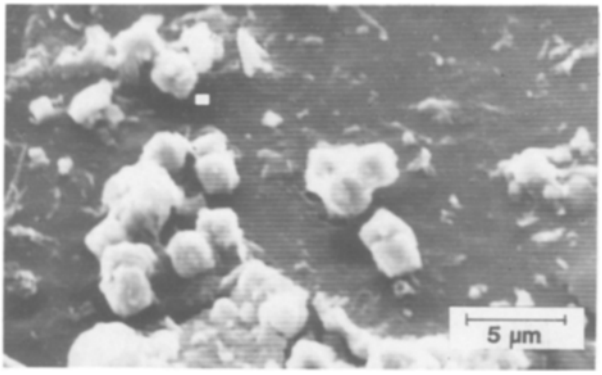

Figure 5 Pyrites crystals on the exposed surface of the corrosion crust from specimen DS4.

had basically the same composition. Their regularity indicates a high degree of crystallinity; their composition and habit suggest they are deposits of gypsum, $CaSO_4 \cdot 2H_2O$.

Specimen DS4 also revealed interesting detail. The exposed surface was found to be covered with small regular-shaped objects, a number of which are illustrated in Fig. 4; EPMA showed them to be well-formed crystallites of sulphur. The surface of the crust at the glass–corrosion interface was also of note: in addition to deposits of sulphur, small cubic features occurred – of the order of 2 to 3 μm in size – rich in iron and sulphur (in wt %: Fe 22 to 25, S 30 to 33), suggestive of their being pyrites, FeS_2. Positive identification of these crystals, a number of which are shown in Fig. 5, is discussed in Section 3.4.

Specimens from the *Amsterdam* were also examined in this way. The exposed surface of the crust was relatively flat and covered with a fine fibrous mat, rich in iron but devoid of sulphur. The red–brown colour of this material is suggestive of iron in the ferric state, possibly as the hydroxides $Fe(OH)_3$ or FeOOH. At the interface with the glass, the crust was covered with ridges, as illustrated in Fig. 6; it was essentially featureless on a fine scale. A few crystals of pyrites and sulphur were also present.

3.3. Polished specimens

Examination of polished sections revealed further detail of the morphology of the crusts and on the distribution of elements. The depth profile of elements within the crusts was determined by spot EPMA. The results for specimen DS2 are plotted in Fig. 7, where the main features are the slight enrichment of silica at the glass–corrosion interface, the increased amounts of alumina *vis-à-vis* that in the pristine glass, and the almost complete removal through leaching of the alkali, magnesia and calcia. Iron remained at much the same level as in the glass, except in the proximity of the surface where there was a sharp increase. Sulphur was also concentrated at the surface, as indicated in Table II.

Sectioned specimens from the *Amsterdam* were also examined. Depth profiles of the elements showed the same trends as for the DS material, see Fig. 7.

Fig. 8 shows a section through the corrosion products on specimen AMS6. The laminar structure is visible, although individual layers tend to be more diffuse in the case of marine-corroded glass compared with those we have observed on soil-corroded material. In specimens from both sources the layers mostly ran parallel to the original surface of the glass and were continuous, indicating that they were formed consecutively and discretely, as will be further elaborated upon in Section 4. The layered corrosion crust on AMS6 is also evident in Fig. 9, and whereas in most regions a smooth, regular, growth pattern had developed, in others the layers were folded or otherwise contorted. Similar features in naturally corroded glass have been reported by other investigators [2–5]. The

TABLE II Composition of the corrosion products

Oxide	*Amsterdam*				*Drottengin af Sverige*			
	AMS1		AMS3		DS1		DS4	
	Exposed surface	Interface	Exposed surface	Interface	Exposed surface	Interface	Exposed surface	Interface
Na_2O	2.3	2.8	2.6	2.5	3.6	7.7	7.9	5.3
MgO	0.2	0.4	0.1	0.2	0.5	0.9	0.6	0.5
Al_2O_3	9.6	10.3	10.1	9.7	14.8	15.1	9.9	14.4
SiO_2	68.5	77.8	66.0	81.9	56.7	60.1	48.3	67.7
P_2O_5	0.5	0.1	0.2	ND	0.6	0.1	0.2	0.1
K_2O	3.1	2.8	3.3	2.4	4.0	5.0	4.4	5.1
CaO	0.4	0.4	0.9	0.3	0.9	0.6	6.8	0.5
MnO	ND	0.1	ND	ND	0.2	0.1	0.1	0.1
Fe_2O_3	7.4	0.6	1.5	0.3	1.3	1.3	1.4	1.0
S	0.4	0.2	0.7	0.2	1.1	0.3	7.0	0.6

ND Not detected.

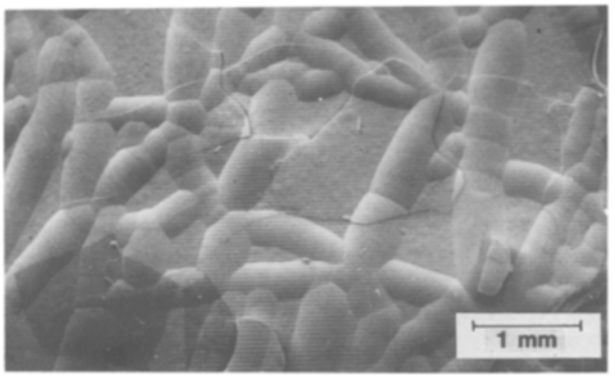

Figure 6 Surface of the corrosion crust at the glass–corrosion interface, from specimen AMS1.

reason for their formation is far from clear, but in this example they may be the result of surface microcracks, inhomogeneties or irregularities which have served to distort the shape of the advancing corrosion front [10]. Inclusions, too, influence the smooth progression of the front, as may be seen in Fig. 10 where the remains of a gas bubble, present in the original glass, has disturbed the contours of the corrosion layers. They have curved around the void and "fanned out" as the corrosion front advanced past the bubble. The junction between the parallel layers and those curving around the bubble is sharp; individual layers remain continuous, as may be seen in Fig. 11. These features are important for two reasons. First, the form of the layers shows that bubbles within glass do not act as nuclei for corrosion, as there is no sign of the corrosion front having advanced outwards from the void towards the original surface. Second, such features serve to explain the blisters, approximately hemispherical in shape, seen on the surface of the corrosion crust adjoining the glass.

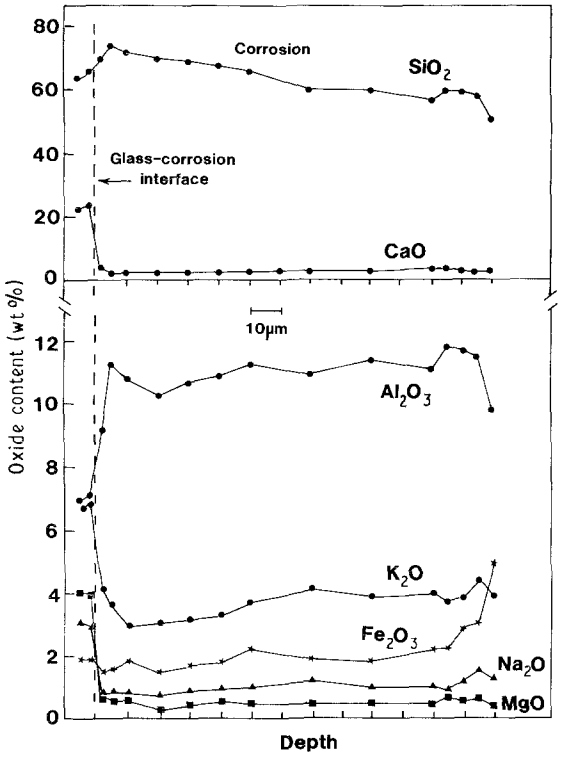

Figure 7 Depth profiles of the elements in the glass and corrosion crust on specimen DS2.

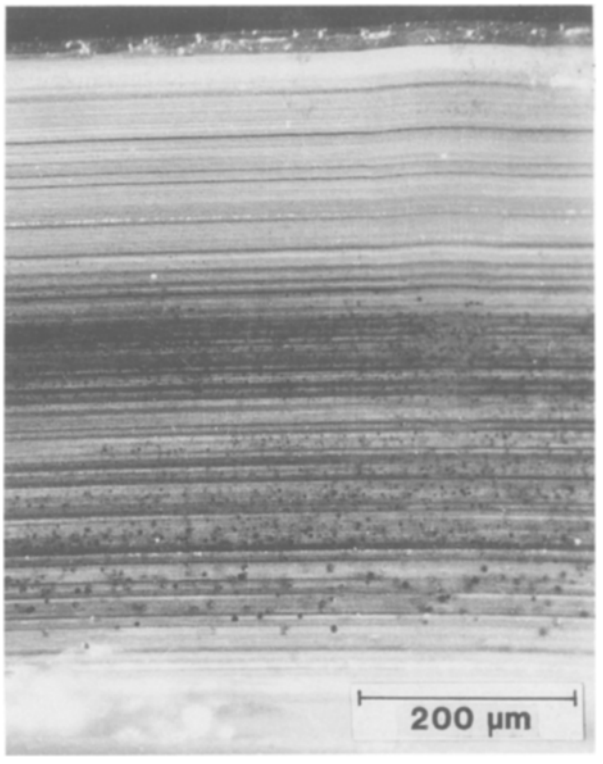

Figure 8 Optical micrograph of a section of specimen AMS6 showing the regular layer structure of the crust. The dark inclusions are pyrites.

Inclusions of a different type in material from the *Amsterdam* are shown in Fig. 11 where they appear as light areas against the darker background. At somewhat higher magnifications, many such inclusions up to about 10 μm in size were seen to be incorporated into the crust. Their presence did not distort the local layer structure, as may be seen in Fig. 12. EPMA revealed them to be rich in iron and sulphur and they are almost certainly further deposits of pyrites. Individual layers pass through the inclusions, showing they had been co-precipitated with the material forming the layers, and were not simply trapped particles.

3.4 Diffraction and infrared absorption

The results of electron and X-ray diffraction studies of the corrosion products supported, in part, those

Figure 9 Optical micrograph of a section of specimen AMS6 showing a distorted region of the crust.

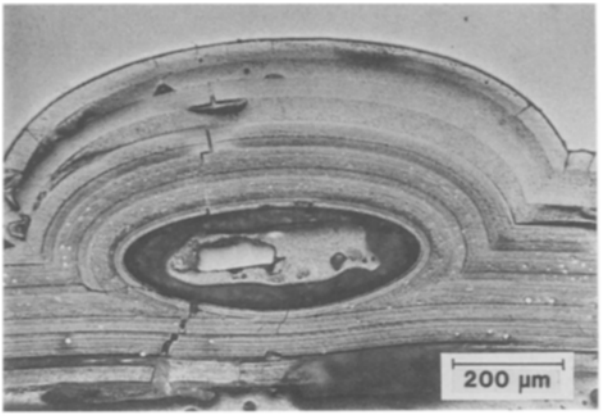

Figure 10 Optical micrograph of a section of specimen AMS4. The corrosion front (at the top of the picture) has passed through a bubble present in the original glass.

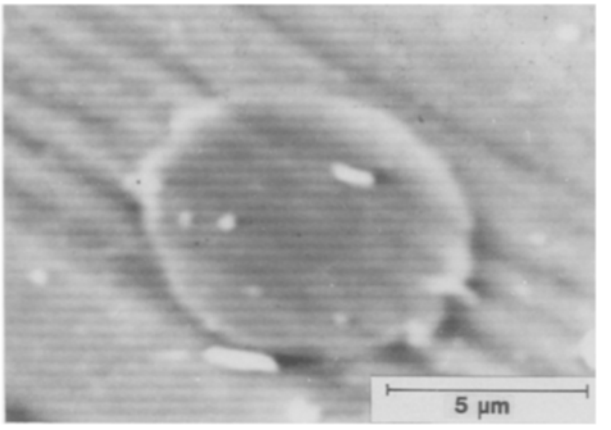

Figure 12 Scanning electron micrograph of a pyrites inclusion in specimen AMS6. The layer structure of the corrosion crust passes through the inclusion.

obtained by EPMA. Samples from the *Amsterdam* produced electron diffraction spot patterns corresponding to localized deposits of pyrites, FeS_2. X-ray diffraction, however, provided evidence for crystalline phases which were not detected by EPMA, namely potassium lead silicate, $K_2Pb_2Si_2O_7$, in specimen DS1, and iron magnesium hydroxide, $(FeMg)(OH)_2$ in AMS1 and AMS4. Closer examination of *Drottengin af Sverige* material using EPMA revealed one area where lead and potassium were concentrated, but no further identification was possible. As a general statement, the degree of crystallinity of the corrosion products was extremely low.

The infrared absorption spectra of the glass and the crust from specimen DS1 are shown in Fig. 13; for comparison that of fused silica is also included. There is much in common to the three spectra. The strong absorption band in the region of 1000 to 1100 cm^{-1}, corresponding to the O–Si–O fundamental stretching vibration [11, 12] is prominent and verifies that the corrosion crust has a bonded silicon–oxygen structure. For fused silica this band is centred at 1100 cm^{-1}, but for the glass it is considerably broadened, reduced in intensity and shifted to lower wavenumbers, trends which have been associated with the break-up of the Si–O network and a weakening of the bonding [13].

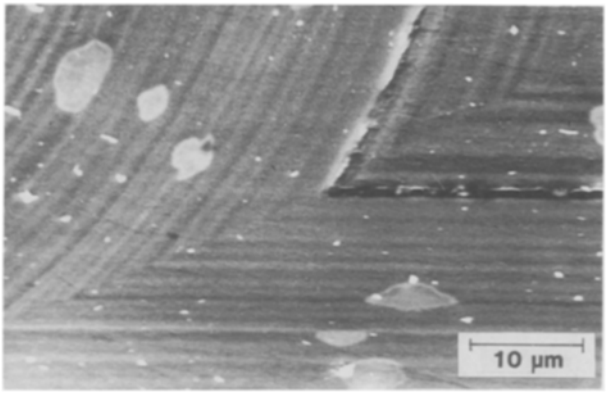

Figure 11 Scanning electron micrograph of a detail of Fig 10 showing the junction between the parallel and curved layers. The light areas are inclusions of pyrites.

Compared with the spectrum of the glass, that of the corrosion shows a narrower absorption near 1050 cm^{-1}, presumably a consequence of the reduced concentrations of ionic species in the leached surface layers. A weaker band is present in the spectrum of the corrosion near 920 cm^{-1} (barely discernible in that of the glass on account of its inclusion in the broad absorption centred near 1020 cm^{-1}) and entirely absent from that of fused silica. We have observed a stronger, corresponding feature at 940 cm^{-1} in the spectrum of muscovite mica; it has also been reported in that of kaolinite [14]. Both materials have sheet silicate structures. This absorption has been attributed to stretching modes of non-bridging oxygen groups, namely $Si–O^-$ [12, 13].

The absorption bands near 790 and 480 cm^{-1} – prominent in the spectrum of silica, but greatly modified in that of the glass – are attributed to stretching and bending modes, respectively, of the silica network [15].

The infrared spectra of the glass and corrosion products from AMS specimens very closely resembled those shown in Fig. 13.

4. Discussion

The hydrolytic attack of alkali-lime-silicate glasses has been extensively studied [16]. Initially, alkali ions, R^+, are released into solution as a consequence of ion exchange; protons, H^+, or more probably hydronium ions, H_3O^+ [17], enter the glass resulting in the formation of a leached, hydrated layer

$$\equiv Si–OR + H_2O \rightleftharpoons \equiv Si–OH + R^+ + OH^- \ldots \quad (1)$$

This layer reduces the rate of alkali extraction by forming a surface barrier through which alkali ions must diffuse in order to enter into solution. The network of the glass remains intact during this process.

Hydroxyl ions, OH^-, in solution attack the siloxane bonds in the glass network

$$\equiv Si–O–Si \equiv + OH^- \rightleftharpoons \equiv Si–OH + \equiv Si–O^- \ldots \quad (2)$$

The non-bridging oxygens formed in Reaction 2 can interact with water to form further silanol bonds and

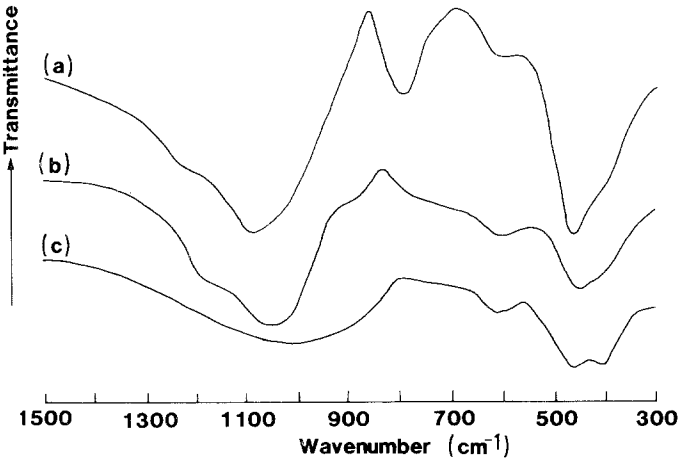

Figure 13 Infrared transmission spectra of: (a) fused silica, (b) corrosion from specimen DS1, and (c) pristine glass from specimen DS1.

release hydroxyl ions

$$\equiv Si\text{-}O^- + H_2O \rightleftharpoons Si\text{-}OH + OH^- \quad (3)$$

The hydroxyl ions freed in Reaction 3 are available to repeat Reaction 2, the net result being the destruction of the silica network of the glass. Solutions with pH values $\geqslant 9$ favour network dissolution [18].

The corrosion of glass in a marine environment is more complex than is suggested above; salts in solution, the presence of sediments, dissolved gases and organic matter may all influence chemical processes. That ion exchange has taken place in the surface regions of the specimens we have examined is evident from Fig. 7, where the monovalent (Na^+, K^+) and divalent (Ca^{2+}, Mg^{2+}) cations are much reduced in concentration at the glass–corrosion interface and in the crusts. Similar findings were reported by Lutze *et al.* [19] who analysed a natural basaltic glass which had been in contact with seawater for geological periods of time. However, in Brill and Moll's report [20] of a specimen of glass, similar in composition to the AMS glasses, recovered from the sea bed off Port Royal, Jamaica, they observed that although calcium had been leached from the surface, it had been replaced by magnesium on an almost equi-molar basis. Ion-exchange with the marine sediment was put forward as a possible explanation.

Seawater itself presents a mildly alkaline environment, its pH value generally lying within the range 7.8 to 8.2 [21], although more extreme conditions may occur in sediments. However, in the case of poorly durable glass which develops a relatively thick corrosion crust, the pH of the environment is unlikely to be the dominant factor which determines the final outcome of corrosion processes. As ion-exchange proceeds, the flow rate of the attacking solution within the leached regions will be restricted – the thicker the surface layers, the more static will be the solution at the corrosion front. Consequent upon Reaction 2, the local pH of this solution will increase until it reaches a value sufficient for network dissolution to occur.

Where it was certain that the corrosion crusts had been preserved intact, their thickness varied between about 350 and 600 μm. The mean layer separation was 2 μm. Thus within the complete crusts there were some 175 to 300 individual layers (average 238) on glass which had been submerged for about 240 years. Brill and Hood [5] proposed that regular layer structures of this type were caused by periodic variations in the temperature or water content of the environment, one layer being formed *per annum*. It would appear that our data support their suggestion, but in common with Newton [4] we believe this to be fortuitous. In the case of marine corrosion, where temperature variations are small and water is always present, it is difficult to accept that seasonal variations are responsible for layer formation. Significantly, Raw [2] observed that laminated crusts could be produced by exposing glass to constant hydrothermal conditions, a fact confirmed by more recent investigators.

The crusts we have examined readily cleave along the planes of the layers; with care they may be removed with a scalpel. The combined SEM, EPMA and infrared results suggest that the corrosion products have a sheet silicate structure containing alumina and a range of cations. Layer formation may take place as follows: at pH values $\geqslant 9$, glass network dissolution occurs then, as solubility limits of oxides in solution are exceeded, new solid phases (as yet unidentified) are precipitated which regulate the pH and concentration of the solution at the corrosion front. Thus cyclic reaction kinetics will prevail. The porous nature of the layers facilitates the diffusion of the leachant and the migration of leached ions through the crust. A similar reaction mechanism has been put forward by Grambow [22] to account for the dissolution of nuclear waste glasses. Murakami and Banba [23], in their study of leached nuclear waste glasses, identified a sheet silicate of chemical type $A_xB_y(SiAl)_z(OH)_m$, where A and B denote a variety of cations located at two different specific sites.

That total breakdown of the glass network (congruent dissolution) had occurred in the specimens we examined, followed by precipitation of new phases, is verified by the internal structure of the FeS_2 particles in the crusts on AMS material. These inclusions were not simply present as "captured" particles, but formed an integral part of the layers, as described in Section 3.3. Had complete breakdown of the glass network not occurred, the presence of such particles would have distorted the parallelism of the layers. In contrast to the above, the research of Dran *et al.* [24] into the accelerated aqueous corrosion of borosilicate glasses containing fission tracks some 5 to 10 nm diameter,

revealed that the hydrated surface layer, about 1 μm thick, embodied relics of the tracks, showing that complete dissolution of these glasses could not have taken place.

The crystalline phases we have identified on the corroded surfaces are largely of uncertain origin. In the case of $CaSO_4 \cdot 2H_2O$, for example, the sulphate ion is undoubtedly derived from seawater, whereas the calcium ion could be from either the glass or the seawater. Only in the case of silicon in $K_2Pb_2Si_2O_7$ is it reasonably certain that this component is from the glass.

There are several reports of crystalline products on the surfaces of glasses corroded in the laboratory under hydrothermal conditions. The mixed hydroxide $(FeMg)(OH)_2$ has also been detected on a basaltic glass [25], as has analcime, $NaAlSi_2O_6 \cdot H_2O$ [26], and hydrotalcite, $Mg_6Al_2CO_3(OH)_{16} \cdot 4H_2O$ [25]. Tobermorite, $Ca_5(OH)_2Si_6O_{16} \cdot 4H_2O$, has been reported on a corroded borosilicate glass [27]. Gibbsite, $Al(OH)_3$, and pyrophyllite, $Al_2Si_4O_{10}(OH)_2$, have both been identified amongst the alteration products on aluminosilicate glasses [28]. With one exception, namely iron magnesium hydroxide, none of these compounds were observed in the present work. Whilst this may partly be accounted for by the different compositions of the glasses we have examined, it may also be due to the normally much lower temperatures at which corrosion proceeds in the natural environment.

The bacterial reduction of sulphates in seawater and sediments to hydrogen sulphide is well known [29], and hence the production of metal sulphides. The presence of FeS_2 within the crusts on AMS material may seem anomalous when iron, seemingly in the ferric state, also appears in surface precipitates. However, Kaplan and Rittenberg [30] have suggested that micro-environments adequate for reducing sulphates can occur in a milieu that is predominantly oxidizing. Accounting for the presence of crystalline sulphur is more problematic: presumably it is either the final stage in the reduction of sulphates, or it may possibly be formed from hydrated iron monosulphide, which is unstable and decomposes to iron oxides and sulphur on drying [30, 31].

5. Conclusion

The natural corrosion of glass recovered from the sea bed at two UK in-shore sites has been shown to involve the processes of hydration, ion-exchange and hydroxyl-ion attack on the glass network. For alkali-lime-silicate glasses of the type investigated, congruent dissolution of the glass occurs. New solid phases are precipitated in the form of well-developed surface layers, which may show considerable structural complexity, as a consequence of cyclic reaction conditions at the corrosion front.

The crystalline compounds which are present amongst the corrosion products originate only in part from the decomposition of the glass. In general, they differ from the phases which have been identified on the surface of basaltic and man-made glasses subjected to hydrothermal conditions in the laboratory. Thus, whilst short-term studies of the corrosion of glasses at elevated temperatures and pressures provide data relevant to the initial "thermal-period" in a nuclear waste repository, such data may not be representative of the conditions that prevail during the "post-thermal-period" – which may be of several thousand years' duration [26]. It is to this latter period that the study of the long-term natural corrosion of glass may be most applicable.

Acknowledgements

We thank Mr J. C. and Mrs L. Joffre for kindly providing specimens of glass recovered from the *Drottengin af Sverige* and Mr A. Williamson of the Shetland Islands Museum for permission to publish details of our findings on this material. Similarly, we are indebted to Dr J. H. G. Gawronski, Coordinator of the *Amsterdam* Project, and to Miss C. Giangrande for bringing to our notice glass recovered from the VOC-Schip *Amsterdam* and for generously providing specimens of the same. Mr N. M. Rudman of the Department of Physics, University of York, carried out the diffraction studies; Mr S. Moehr, also of this Department, kindly polished the sectioned specimens. Finally, we are indebted to Dr R. M. Perutz of the Department of Chemistry, University of York, for help and advice on infrared spectroscopy.

References

1. D. BREWSTER, *Phil. Trans. R. Soc. Edin.* **23** (1863) 193.
2. F. RAW, *J. Soc. Glass Technol.* **39** (1955) 128T.
3. W. GEILMANN, *Glastech. Ber.* **29** (1956) 145.
4. R. G. NEWTON, *Archaeometry* **13** (1971) 1.
5. R. H. BRILL and H. P. HOOD, *Nature* **189** (1961) 12.
6. I. FRIEDMAN and F. W. TREMBOUR, *Amer. Scientist* **66** (1978) 44.
7. R. B. HEIMANN, *Glass Technol.* **27** (1986) 96.
8. S. KENTIE, in Annual Report of the VOC Schip "Amsterdam" Foundation 1985, edited by J. H. G. Gawronski (Amsterdam, 1986) p. 51.
9. G. LOVE, in "Quantitative Electron-Probe Microanalysis" edited by V. D. Scott and G. Love (Ellis Horwood, Chichester, 1983) p. 234.
10. J. F. FLINTOFF and A. B. HARKER, *Mater. Res. Soc. Sym. Proc.* **44** (1985) 147.
11. I. SIMON and H. O. McMAHON, *J. Amer. Ceram. Soc.* **36** (1953) 160.
12. *Idem, J. Chem. Phys.* **21** (1953) 23.
13. P. E. JELLYMAN and J. P. PROCTER, *J. Soc. Glass Technol.* **39** (1955) 173T.
14. R. P. NYQUIST and R. O. KAGEL, in "Infrared Spectra of Inorganic Compounds" (Academic, New York, 1971) spectrum no. 95.
15. E. A. LIPPINCOTT, A. V. VALKENBURG, C. E. WEIR and E. N. BUNTING, *J. Res. Nat. Bur. Stand.* **61** (1958) 61.
16. A. PAUL, in "Chemistry of Glasses" (Chapman and Hall, London, 1982) p. 109.
17. R. H. DOREMUS, *J. Non-Cryst. Solids* **19** (1975) 137.
18. R. W. DOUGLAS and T. M. M. EL-SHAMY, *J. Amer. Ceram. Soc.* **50** (1967) 1.
19. W. LUTZE, G. MALOW, R. C. EWING, M. J. JERCINOVIC and K. KEIL, *Nature* **314** (1985) 252.
20. R. H. BRILL and S. MOLL, in "Recent Advances in Corrosion" edited by G. Thompson (Butterworths, London, 1963) p. 145.
21. J. P. RILEY and R. CHESTER, in "Introduction to Marine Chemistry" (Academic, London, 1971) p. 120.
22. B. GRAMBOW, in Proceedings of the Materials Research Society 5th International Symposium on the Scientific Basis for Nuclear Waste Management, Berlin, June 1982, edited by W. Lutze (Elsevier Science, New York, 1982) p. 93.

23. T. MURAKAMI and T. BANBA, *Nucl. Technol.* **67** (1984) 419.
24. J.-C. DRAN, J.-C. PETIT and C. BROUSSE, *Nature* **319** (1986) 485.
25. G. EHRET, J. L. CROVISIER and J. P. EBERHART, *J. Non-Cryst. Solids* **86** (1986) 72.
26. G. MALOW, W. LUTZE and R. C. EWING, *ibid.* **67** (1984) 305.
27. J. K. BATES, L. J. JARDINE and M. J. STEINDLER, *Science* **218** (1982) 51.
28. C. M. JANTZEN and M. J. PLODINEC, *J. Non-Cryst. Solids* **67** (1984) 207.
29. J. P. RILEY and R. CHESTER, in "Introduction to Marine Chemistry" (Academic, London, 1971) p. 115.
30. I. R. KAPLAN and S. C. RITTENBERG, in "The Sea", Vol. 3, edited by M. N. Hill (Wiley, New York, 1963) p. 609.
31. E. W. GALLACHER, *J. Sed. Petrol.* **3** (1933) 51.

Received 15 August
and accepted 30 November 1988